Biogeosciences Discuss., 12, 2745–2786, 2015
www.biogeosciences-discuss.net/12/2745/2015/
doi:10.5194/bgd-12-2745-2015

Biogeosciences
Discussions
Open Access

Modelling the climatic drivers determining photosynthesis and carbon allocation in evergreen Mediterranean forests using multiproxy long time series

G. Gea-Izquierdo[1], F. Guibal[2], R. Joffre[3], J. M. Ourcival[3], G. Simioni[4], and J. Guiot[1]

[1]CEREGE UMR7330, CNRS/Aix-Marseille Université, Europole de l'Arbois BP, 80 13545 Aix-en-Provence cedex 4, France
[2]IMBE, CNRS/Aix-Marseille Université UMR7263, Europole de l'Arbois BP, 8013545 Aix-en-Provence cedex 4, France
[3]Centre d'Ecologie Fonctionnelle et Evolutive CEFE, UMR5175, CNRS – Université de Montpellier – Université Paul-Valéry Montpellier – EPHE, 1919 Route de Mende, 34293 Montpellier CEDEX 5, France
[4]Ecologie des Forêts Méditerranéennes, INRA UR629, Domaine Saint Paul, 84914 Avignon CEDEX 9, France

Received: 28 December 2014 – Accepted: 23 January 2015 – Published: 6 February 2015

Correspondence to: G. Gea-Izquierdo (gea-izquierdo@cerege.fr)

Published by Copernicus Publications on behalf of the European Geosciences Union.

Abstract

Climatic drivers limit several important physiological processes involved in ecosystem carbon dynamics including gross primary productivity (GPP) and carbon allocation in vegetation. Climatic variability limits these two processes differently. We developed an existing mechanistic model to analyse photosynthesis and variability in carbon allocation in two evergreen species at two Mediterranean forests. The model was calibrated using a combination of eddy covariance CO_2 flux data, dendrochronological time series of secondary growth and forest inventory data. The model was modified to be climate explicit in the key processes addressing acclimation of photosynthesis and allocation. It succeeded to fit both the high- and the low-frequency response of stand GPP and carbon allocation to the stem. This would support its capability to address both carbon source and sink limitations. Simulations suggest a decrease in mean stomatal conductance in response to environmental changes and an increase in mean annual intrinsic water use efficiency (iWUE) in both species during the last 50 years. However, this was not translated on a parallel increase in ecosystem water use efficiency (WUE). A long-term decrease in annual GPP matched the local trend in precipitation since the 1970s observed in one site. In contrast, GPP did not show a negative trend and the trees buffered the climatic variability observed at the site where long-term precipitation remained stable. In our simulations these temporal changes would be partly related to increasing [CO_2] because the model includes biochemical equations where photosynthesis is directly linked to [CO_2]. Long-term trends in GPP did not match those in growth, in agreement with the C-sink hypothesis. There is a great potential to use the model with abundant dendrochronological data and analyse forest performance under climate change. This would help to understand how different interfering environmental factors produce instability in the climatic signal expressed in tree-rings.

1 Introduction

Global change challenges forest performance because it can enhance forest vulnerability (IPCC 2013). Trees modify multiple mechanisms at different scales to tackle with environmental stress, including changes in photosynthesis and carbon allocation within plants (Breda et al., 2006; Niinemets, 2007; Chen et al., 2013). Many factors affect the different physiological processes driving forest performance. Among them, the net effect of rising [CO_2] and climate change is meaningful to determine the forests' capacity of acclimation to enhanced xericity (Peñuelas et al., 2011; Keenan et al., 2011; Fatichi et al., 2014). Forest process-based models have been developed to mimic these mechanisms. They can include different levels of complexity but generally implement calculations of leaf photosynthesis up-scaled to the canopy and carbon allocated to different plant compartments (Le Roux et al., 2001; Schaefer et al., 2012; De Kauwe et al., 2013). Although there is evidence that the tree performance depends to some extent on stored carbohydrates (Breda et al., 2006; McDowell et al., 2013; Dickman et al., 2014), these models have received some criticism when used to understand plant performance in response to climate change. This is in part because they are C-source oriented, therefore can exhibit certain limitations to represent the C-sink hypothesis and address dysfunctions related to the tree hydraulics (Breshears et al., 2009; Sala et al., 2012; McDowell et al., 2013; Fatichi et al., 2014).

Complex process-based models profit from multiproxy calibration, particularly when such data apply at different spatio-temporal scales (Peng et al., 2011). The temporal scale can be approached using time growth series of dendrochronological data. However the analysis of the past always adds uncertainties related to the influence of unknown stand conditions to properly scale productivity. Flux data including stand productivity can be estimated using the eddy covariance technique (Baldocchi, 2003). These data overcome many of the limitations of dendroecological data (e.g. intra-annual resolution, control of stand conditions and scaling of net productivity) but they lack their spatial and temporal coverage. Thus, CO_2 data can be used to implement unbiased models of photosynthesis, and then combined with dendroecological data to study how carbon is allocated as a function of environmental forcing (Friedlingstein et al., 1999; Chen et al., 2013; McMurtrie and Dewar, 2013).

Mechanistic models can be also used to analyse the environmental factors determining instability in the climate-growth response (D'Arrigo et al., 2008). Different process-based models have been applied with dendroecological data used either in forward or inverse mode (see Guiot et al., 2014 for a review). Among these models, the process-based model MAIDEN (Misson, 2004) was originally developed using dendroecological data. The model explicitly includes [CO_2] to calculate photosynthesis (hence its influence on carbon allocation) and includes a carbohydrate storage reservoir. The latter being one of its strengths compared to other models (Vaganov et al., 2006; Sala et al., 2012; Guiot et al., 2014). It has been previously employed to analyse growth variability in one temperate and two Mediterranean species (Misson et al., 2004; Gaucherel et al., 2008) and recently on inverse mode (also including C and O stable isotopes) to reconstruct past climate (Boucher et al., 2014). However, it requires further development to calculate unbiased estimates of forest productivity and assess uncertainties in the response of trees to climatic variability at a greater scale. Particularly, its parameterization would need improvement whether the model was used to assess hypotheses regarding the implication of climatic factors on performance and C allocation within plants (Niinemets and Valladares, 2004; Fatichi et al., 2014).

In this study we use multiproxy data to develop a process-based model and investigate how evergreen Mediterranean forests have modified stand photosynthesis and carbon allocation in response to interacting climatic factors and enhanced [CO_2] in the recent past. The first objective was to develop a process-based model based on MAIDEN (Misson, 2004). Within the new version of the model, photosynthesis, carbon allocation, canopy turnover and phenology are now calculated using climate explicit functions with a mechanistic basis. The model is adapted to give unbiased estimates of canopy photosynthesis and stem growth using instrumental data. Specifically, within the new model formulation: (1) photosynthesis is penalized by prolonged water stress conditions through reductions in leaf area index (LAI) and maximum photosynthetic capacity, (2) carbon allocation variability is directly determined by soil water content (i.e. water stress) and temperature through nonlinear relationships, (3) these relationships can be contrasted for different phenophases and affect independently photosynthesis and allocation. Once the model was developed, a second objective was to analyse how [CO_2] and climatic variability affect the temporal instability in annual forest productivity, water use efficiency and carbon allocation. We hypothesise that they will exhibit differences in their long-term variability in relation to recent climate change.

2 Material and methods

2.1 Study sites and climatic data

The study sites were two evergreen Mediterranean monitored forests in Southern France where CO_2, water vapour and energy fluxes are measured using the Eddy covariance technique (Baldocchi, 2003). Both sites are included in FLUXNET (http://fluxnet.ornl.gov/). The first site Fontblanche (43.2° N, 5.7° E, 420 m) is a mixed stand where *Pinus halepensis* Mill. dominates the open top canopy layer reaching about 12 m, *Quercus ilex* L. forms a lower canopy layer reaching about 6 m and there is a sparse shrub understory including *Quercus coccifera* L. (Simioni et al., 2013). The second site, Puechabon (43.4° N, 3.4° E, 270 m), is a dense coppice which overstory is dominated by *Q. ilex* with density around 6000 stems ha^{-1} (Rambal et al., 2004; Limousin et al., 2012). Both forests grow on rocky and shallow soils with low retention capacity and of Jurassic limestone origin. The climate is Mediterranean, with a water stress period in summer, cold or mild winters and most precipitation occurring between September and May. Meteorological data were obtained from the neighbouring stations of St. Martin de Londres (for Puechabon) and Aubagne (for Fontblanche). According to those data Puechabon is colder and receives more precipitation than Fontblanche (Table 1). Meteorological data showed a decrease in total rainfall since the 1960s in

Puechabon but no trend in Fontblanche. Both sites exhibit a positive trend in temperatures more evident for the maximum values (Fig. A1).

We assumed that GPP is driven by the top pine and/or oak layers and that the percentage of LAI related to the understory shrub layer will behave like that of the oak species (evergreen, shrubby). For Fontblanche we considered a maximum leaf area index ($\mathrm{LAI_{max}}$) of 2.2 $\mathrm{m^2\,m^{-2}}$ (3 $\mathrm{m^2\,m^{-2}}$ plant area index, PAI), composed by a 70 % of pine and 30 % of oak (Simioni et al., 2013). For Puechabon we considered a $\mathrm{LAI_{max}}$ of 2.0 $\mathrm{m^2\,m^{-2}}$ (2.8 $\mathrm{m^2\,m^{-2}}$ PAI) monospecific of *Q. ilex* (Baldocchi et al., 2010; Limousin et al., 2012). Specific leaf area (SLA) considered was 0.0045 $\mathrm{m^2\,g^{-1}}$ for *Q. ilex* and 0.0037 $\mathrm{m^2\,g^{-1}}$ for *P. halepensis,* respectively (Hoff and Rambal, 2003; Maseyk et al., 2008).

2.2 The model

We used MAIDEN (Misson, 2004), a stand productivity mechanistic model driven by a number of functions and parameters representing different processes. The model inputs are precipitation, maximum and minimum temperature and CO_2 with a daily time step. This model has been previously implemented for monospecific forests including two oaks and one pine species using dendroecological chronologies of growth and, when available, stand transpiration estimates from sap-flow sensors (Misson et al., 2004; Gaucherel et al., 2008). However, the model has never been compared to actual CO_2 data to ensure that it provides unbiased estimates of stand productivity. In this study, the model was further developed to match ground-based observations and generalize model use by modifying the photosynthesis and allocation modules (including the different phenophases) in relation to climatic drivers. To properly scale model outputs and get unbiased estimates of stand productivity we used CO_2 eddy covariance data (Baldocchi, 2003). Different parameters were calibrated to different data sources, including some species-dependent and some site-dependent parameters, as follows. Those equations used to calculate micrometeorological covariates, soil humidity and photosynthetic active radiation, as well as those functions describing the water cycle (including soil evaporation and plant transpiration) are explained in the original model formulation from Misson (2004). Therefore they won't be described here. The rest of the model was modified as follows.

2.3 Modelling the effect of climatic forcing on photosynthesis

Leaf photosynthesis (A_n) is calculated based on the biochemical model of Farquhar et al. (1980). A_n is a function of the carboxylation (V_c), oxygenation (V_o) and dark respiration rates (R_d): $A_n(i) = V_c - 0.5V_o - R_d$; where photosynthesis at day i is limited by either the rate of carboxylation when Rubisco is saturated (W_c) or when it is limited by electron transport (W_j), i.e. $A_c = V_c - 0.5V_o = \min\{W_c, W_j\}$. R_d was considered a fixed function of A_c ($0.006 \cdot A_c$), because it performed better in our daily model than exponential formulations as a function of temperature (Sala and Tenhunen, 1996; De Pury and Farquhar, 1997; Bernacchi et al., 2001). Following De Pury and Farquhar (1997):

$$W_c(i) = \frac{V_{\mathrm{cmax}}(i) \cdot (C_i(i) - \Gamma(i))}{C_i(i) + K_o(i)\left(1 + \frac{[\mathrm{O_2}]}{K_o(i)}\right)}, \tag{1}$$

$$W_j(i) = \frac{J_{\max}(i) \cdot (C_i(i) - \Gamma(i))}{4C_i(i) + 8\Gamma(i)}; \tag{2}$$

where C_i is the $\mathrm{CO_2}$ intercellular concentration, Γ is the [$\mathrm{CO_2}$] compensating point for photosynthesis in the absence of dark respiration, and K_c and K_o are the kinetic Michaelis–Menten constants for carboxylation and oxygenation, respectively. V_{cmax} and $J_{\max}$ are temperature dependent parameters as follows.

Climate influences leaf photosynthesis calculations through the temperature dependence of different parameters (Bernacchi et al., 2001; Nobel, 2009). Γ, K_c and K_o were modelled using Arrhenius functions of daily mean temperature (T_{day}, in °C) with parameters as in De Pury and Farquhar (1997). We modelled $J_{\max}$ as a fixed rate of V_{cmax} ($J_{\max}(i) = J_{coef} \cdot V_{\mathrm{cmax}}(i)$) after comparing with different temperature dependent formulations (De Pury and Farquhar, 1997; Maseyk et al., 2008). The temperature dependence of V_{cmax} behaved better when modelled using a logistic function (Gea-Izquierdo et al., 2010) rather than an exponential function as in Misson (2004):

$$V_{\mathrm{cmax}}(i) = \frac{V_{\mathrm{max}}}{(1+\exp(V_b \cdot ((T_{\mathrm{day}}(i)+273) - V_{\mathrm{ip}})))} \cdot \theta_{\mathrm{p}}; \tag{3}$$

V_{max}, V_b and V_{ip} are parameters to be estimated, with V_{max} being the asymptote and V_{ip} the inflection point. θ_{p} is a soil water stress function dependent on soil moisture conditions of the previous year. It takes into account the negative effect of protracted drought on the photosynthetic capacity of active LAI in evergreen species caused by constraints in V_{cmax} produced by irreversible photoinhibition, modifications in leave stoichiometry and/or aging of standing foliage through lower leave replacement rates in response to long-term water stress (Sala and Tenhunen, 1996; Niinemets and Valladares, 2004; Niinemets, 2007; Vaz et al., 2010).

$$\theta_{\mathrm{p}} = 1 - \exp(p_{\mathrm{str}} \cdot \mathrm{SWC}_{180}), \tag{4}$$

where p_{str} is a parameter to be estimated and SWC_{180} is the mean soil water content (mm) from July to December of the previous year.

Photosynthesis is coupled to stomatal conductance calculation, which is estimated using a modified version of the Leuning (1995) equation:

$$g_{\mathrm{s}}(i) = \frac{g_1 \cdot A_n(i)}{(C_{\mathrm{s}}(i) - \Gamma(i)) \cdot \left(1 + \mathrm{VPD}(i)/\mathrm{VPD}_0\right)} \cdot \theta_{\mathrm{g}}(i), \tag{5}$$

g_1 and VPD_0 are parameters, $\mathrm{VPD}(i)$ is daily vapour pressure deficit, C_{s} is the surface $[\mathrm{CO_2}]$; θ_{g} is a non-linear soil water stress function as:

$$\theta_{\mathrm{g}}(i) = \frac{1}{1+\exp(\mathrm{soil}_b \cdot (\mathrm{SWC}(i) - \mathrm{soil}_{\mathrm{ip}}))}, \tag{6}$$

soil_b and soil_ip are parameters and SWC(i) is daily soil water content (mm). θ_g accounts for variability in gas exchange under drought conditions which cannot be taken into account only through stomatal control, e.g. related to mesophyll conductance or stomatal patchiness (Reichstein et al., 2002; Grassi and Magnani, 2005; Flexas et al., 2006). The coupled photosynthesis-stomatal conductance system of equations was estimated separately for sun and shade leaves. Canopy photosynthesis was integrated using LAI divided into its sunlit and shaded fractions (De Pury and Farquhar, 1997). Transmission and absorption of irradiance was calculated following the Beer–Lambert law as a function of LAI, with $\text{LAI}_\text{sun} = (1 - \exp(-K_\text{b} \cdot \text{LAI})) \cdot K_\text{b}$ (K_b is the beam light extinction coefficient) and $\text{LAI}_\text{shade} = 1 - \text{LAI}_\text{sun}$ (Misson, 2004). In the mixed stand (Fontblanche), photosynthesis was calculated separately for *Q. ilex* and *P. halepensis*, and then integrated to get stand estimates.

2.4 Modelling the effect of climatic forcing on carbon allocation

The model allocates daily carbon assimilated either to the canopy, stem, roots or storage of non-structural carbohydrates (NSC) to mimic intra-annual carbohydrate dynamics (Misson, 2004; Dickman et al., 2014). Tree autotrophic respiration (R_a) is modelled as a function $f(i)$ of daily photosynthesis and maximum daily temperature (T_max) (Sala and Tenhunen, 1996; Nobel, 2009) as:

$$R_a(i) = \max\{0.3, f(i)\},\ \text{with}\ f(i) = 0.47 \cdot A_n(i) \cdot (1 - \exp(p_\text{respi} \cdot T_\text{max}(i)); \tag{7}$$

where p_respi is a parameter. Net photosynthesis is calculated for day i as $A_\text{N}(i) = A_n(i) - R_a(i)$. The model simulates several phenological phases along the year (see Fig. 1):

[P1] winter period where all photosynthates assimilated daily $A_\text{N}(i)$ are allocated to the storage reservoir (NSCs) but there is no accumulation of growing degree days (GDD),

- [P2] winter period where all A_N (i) are allocated to storage (i.e. the same as in [P1]) but in opposition to [P1] there is active accumulation of GDD which define the threshold GDD_1 to trigger the next phenophase [P3] (budburst, leaf-flush),
- [P3] budburst, where carbon available $C_T(i) = A_\mathrm{N}$ (i)+C_bud (C_bud is daily C storage utilized from buds, a parameter) is either allocated to the canopy, to roots or to the stem,
- [P4] once the canopy has been completed in [P3], then the next phenophase [P4] starts where daily photosynthates A_N (i) are allocated either to the stem or to storage,
- [P5] the last phenophase [P5] starts when the photoperiod (parameter) crosses a minimum threshold in fall. In this phase root mortality occurs. Otherwise [P5] is similar to [P1] and [P2], in the sense that all A_N (i) is used for storage until next year [P3] starts.

Allocation of carbon to different plant compartments is complex because it can be decoupled from photosynthetic production depending on different factors, some of them climatic, acting at different temporal scales (Friedlingstein et al., 1999; Sala et al., 2012; Chen et al., 2013; McMurtrie and Dewar, 2013). In this new version of the model we set the different allocation relationships as nonlinear functions of temperature and soil water content, $h(i) = f_1(T_\mathrm{max}) \cdot f_2(SWC)$, in [P3] and [P4]. This means that now we take into account homeostatic acclimation processes at the canopy level related to LAI dependence on water availability (Hoff and Rambal, 1993; Sala and Tenhunen, 1996; Reichstein et al., 2003). LAI is negatively related to long-term drought because litterfall is negatively linked to water stress (Limousin et al., 2009; Misson et al., 2011) and bud size depends on climate influencing the period of bud formation (Montserrat-Marti et al., 2009). Therefore the actual carbon that can be allocated to the canopy in [P3] of year j ($\mathrm{AlloC}_\mathrm{canopy}(j)$) was set as a function of previous year moisture conditions ($\theta_\mathrm{LAI}(j)$), and maximum carbon that can be allocated to the canopy ($\mathrm{MaxC}_\mathrm{canopy}$).

$\mathrm{MaxC_{canopy}}$ is calculated from $\mathrm{LAI_{max}}$ and SLA, and $\mathrm{AlloC_{canopy}}(j) = \theta_{\mathrm{LAI}}(j) \cdot \mathrm{MaxC_{canopy}}$, where:

$$\theta_{\mathrm{LAI}}(j) = (1 - 2 \cdot \frac{p_{\mathrm{LAI}} - \mathrm{SWC}_{250}}{p_{\mathrm{LAI}}}),\ \text{constrained to } \theta_{\mathrm{LAI}}(j) \in [0.7, 1.0] \tag{8}$$

p_{LAI} is a parameter to be calibrated, SWC_{250} is mean soil water content as calculated by the model (Misson, 2004) for May–December of previous year.

Leaf turnover is variable within years and partly related to water availability (Limousin et al., 2009, 2012). We considered a mean leave turnover rate of 3 years for pines and 2 for oaks. To model within year variability in leave phenology (i.e. leaf growth and litterfall) we followed Maseyk et al. (2008) and Limousin et al. (2009) (Fig. 1). Allocation to the canopy in [P3] is calculated as: $C_{\mathrm{canopy}}(i) = C_T(i) \cdot (1 - 0.2 \cdot h_{3\_1}(i)) \cdot \mathrm{Ratio_{root/leaf}}$; $\mathrm{Ratio_{root/leaf}}$ was fixed to 1.5 for both species (Misson et al., 2004; Ourcival, unpublished data), and:

$$h_{3\_1}(i) = (1 - \exp(p_{3\mathrm{moist}} \cdot \mathrm{SWC}(i))) \cdot \left(\exp\left(-0.5 \cdot \left(\frac{T_{\max}(i) - p_{3\mathrm{temp}}}{p_{3\mathrm{sd}}} \right)^2 \right) \right), \tag{9}$$

$p_{3\mathrm{moist}}$, $p_{3\mathrm{temp}}$ and $p_{3\mathrm{sd}}$ are parameters. The carbon allocated to the stem (C_{stem}) in [P3] is $C_{\mathrm{stem}}(i) = C_T(i) \cdot 0.2 \cdot h_{3\_1}(i) \cdot h_{3\_2}(i)$, where:

$$h_{3\_2}(i) = (1 - \exp(\mathrm{st}_{3\mathrm{moist}} \cdot \mathrm{SWC}(i))) \cdot \left(\exp\left(-0.5 \cdot \left(\frac{T_{\max}(i) - \mathrm{st}_{3\mathrm{temp}}}{\mathrm{st}_{3\mathrm{sd\_temp}}} \right)^2 \right) \right); \tag{10}$$

with h_{3_1} (i) as in Eq. (9); $\mathrm{st}_{3\mathrm{moist}}$, $\mathrm{st}_{3\mathrm{temp}}$ and $\mathrm{st}_{3\mathrm{sd\_temp}}$ are parameters. The carbon allocated to roots in [P3] is set complementary to that of the other compartments to close the carbon budget within the tree, i.e.: $C_{\mathrm{roots}}(i) = C_T(i) - C_{\mathrm{stem}}(i) - C_{\mathrm{canopy}}(i)$.

Finally, in [P4] carbon assimilated daily $A_{\mathrm{N}}(i)$ is allocated either to the stem or to storage until changing to [P5]. There since in [P1] and [P2] again all $A_{\mathrm{N}}(i)$ is only allocated to storage until [P3] next year (Misson, 2004). In [P4], the amount of carbon to be allocated to the stem is now also set as a function of climatic forcing:

$C_{\text{stem}}(i) = A_{\text{N}}(i) \cdot (1 - h_4(i))$ and $C_{\text{stor}}(i) = A_{\text{N}}(i) \cdot h_4(i)$, with:

$$h_4(i) = (1 - \exp(\text{st}_{4\text{temp}} \cdot T_{\max}(i))) \cdot \left(\exp\left(-0.5 \cdot \left(\frac{\text{SWC}(i)}{\text{st}_{4sd\_moist}}\right)^2\right)\right); \tag{11}$$

$\text{st}_{4\text{temp}}$ and $\text{st}_{4\text{sd\_temp}}$ are parameters.

2.5 Eddy covariance CO_2 flux and dendrochronological data

The process-based model was calibrated using daily gross primary productivity (GPP), dendrochronological data and inventory data. To develop the model, in a first step those functions used to model daily stand photosynthesis (i.e. Eqs. 1 to 9) were calibrated against GPP values. GPP estimates were obtained from half-hourly net CO_2 measured (NEP). GPP was obtained as the difference between measured net ecosystem productivity and calculated ecosystem respiration (Reichstein et al., 2005). Negative GPP values were corrected following Schaefer et al. (2012). Half-hourly GPP data were integrated to obtain daily estimates for the period 2001–2013 (Puechabon, methods detailed in Allard et al., 2008) and 2008–2012 (Fontblanche) (Table 1).

On a second step, those functions used to model how carbon assimilated and/or storage is allocated to the tree stem (i.e. Eqs. 10 and 11) were developed using calculated annual stem biomass increment time series. Stem biomass increment chronologies were built combining dendroecological data and forest inventory data collected at each site. We built one chronology for *Q. ilex* in Puechabon, a second for *Q. ilex* in Fontblanche and a third one for *P. halepensis* at Fontblanche (Fig. 2). For pines, two perpendicular cores were extracted using an increment borer from 25 trees in fall 2013 whereas for oaks we used crossections. In Fontblanche, 15 oak stems were felled and basal sections collected in spring 2014. A total of 17 oak stems from Puechabon were logged in 2005 and 2008. The age and diameter distributions of the studied forests are depicted in Fig. A2.

All samples were processed using standard dendrochronological methods (Fritts, 1976). Annual growth (RW) was measured using a stereomicroscope and a moving table switched to a computer. RW crossdating was visually and statistically verified. RW estimates were transformed to basal area increments (BAI, $\mathrm{cm}^2\,\mathrm{year}^{-1}$). Mean BAI chronologies were obtained by averaging individual tree BAI time series. In Fontblanche BAI during the period 1987–1995 was standardized relative to the mean calculated after excluding that period (Fig. 2). BAI data were standardized during that period because we did not find a climatic explanation for the abrupt growth peak observed in Fontblanche (Fig. 2). Therefore we assumed that it had been caused by a release event (i.e. reduction in competition) produced by the death of neighbours as a consequence of winter frost during 1985 and 1987 (M. Vennetier, personal communication, 2014). These two frosts were reflected by the presence of characteristic frost rings in most individuals from Fontblanche.

To scale BAI chronologies to the same units as annual stem biomass (which is an output of the model) we used plot inventory data collected around the flux towers at the two sites. Inventory data included stem diameter for all trees and tree height collected for a subsample every two years during 2007–2011 in Fontblanche and annual diameter estimates for the period 1986–2011 for Puechabon. Individual annual biomass increments were estimated by subtracting stem biomass at consecutive years and then stand stem biomass increment (SBI, $\mathrm{g\,C\,m}^2\,\mathrm{year}^{-1}$) built integrating plot data. Stem biomass was calculated using allometric functions. For pines, we calculated stem biomass using diameter and estimated stem height assuming that the tree bole follows a paraboloid shape (Li et al., 2014). For oaks, stem biomass was calculated following Rambal et al. (2004). Once SBI had been estimated for the years we had available inventory data, BAI chronologies were correlatively scaled to SBI units ($\mathrm{g\,C\,m}^2\,\mathrm{year}^{-1}$). We built two mean stand SBI chronologies, one for each site, meaning that we analysed carbon allocation within stands, not differentiating between species in Fontblanche. These two SBI chronologies were used to calibrate sitewise Eqs. (10) and (11).

2.6 Model development and analyses

Parameters were selected according to the ecological characteristics of the species, exploring the model using comprehensive sensitivity analysis to sequentially optimize groups of parameters. In a first step, a group of common parameters (those included in Eqs. 2 to 8) was selected using GPP data from Fontblanche (Table 2). The species-dependent parameters selected for *Q. ilex* in this first step were independently validated when applied in Puechabon (those in Table 2 common for the two sites). In a second step, a subset of site-dependent parameters was calibrated against GPP and SBI data. Four parameters from Eqs. (6) and (9) were calibrated using GPP data, and five parameters in Eqs. (10) and (11) were calibrated using stem biomass increment data (Table 2). The local parameters were calibrated constrained to an ecologically realistic range using a global optimization algorithm and maximum likelihood principles (Gaucherel et al., 2008).

To compare model output with stem biomass chronologies as estimated from dendroecological data we used only the period where we had available daily meteorological data (1960–2013), which was also a period that did not include juvenile years with increasing BAI (BAIs reached an asymptote after increasing the first 15–20 juvenile years, Fig. 2). The model does not take into account how size differences in allometry or ontogeny affect carbon allocation (Chen et al., 2013). We tried to keep the model as simple as possible also because we had no such data to calibrate ontogenic effects. Hence the model is designed for non-juvenile stands with well-coupled canopies that reached their asymptotic $\mathrm{LAI}_{\mathrm{max}}$. For the same reasons it does not take into account how changes in management affect carbon allocation. The model was analysed in terms of goodness of fit. Additionally, for the period where we had available daily meteorological data we simulated time series of GPP, ecosystem water use efficiency (WUE = GPP/ET, with ET = actual evapotranspiration) and intrinsic water use efficiency of sun leaves ($i\mathrm{WUE} = A_\mathrm{N}/g_\mathrm{s}$) calculated following Beer et al. (2009).

3 Results

The studied evergreen forests exhibit a bimodal pattern in GPP with maxima in spring and autumn (Fig. 3) as often observed in Mediterranean ecosystems (e.g. Baldocchi et al., 2010). GPP was above zero almost every day of the year, including winter, particularly in the milder site, Fontblanche (Table 1). This means that there is active photosynthesis all year round in these evergreen forests, including both periods of climatic stress with low temperature and short photoperiod in winter or low moisture availability in summer (Fig. 3). Mean annual GPP was 1431.4 ± 305.4 $\mathrm{g\,C\,m^{-2}\,year^{-1}}$ and precipitation 642.7 ± 169.7 mm in Fontblanche; whereas it was 1207.3 ± 206.7 $\mathrm{g\,C\,m^{-2}\,year^{-1}}$ and 1002.6 ± 328.2 mm in Puechabon (see Table 1 for more details). Mean GPP was higher at Fontblanche because carbon assimilation was greater in the low temperature winter period but similar the rest of the year (Fig. 3). Stem growth did not show any long-term (decadal) growth trend for any of the species studied (Fig. 2).

The model accurately represented the low frequency response of GPP: both the seasonal variability in GPP within years and variability in GPP among years (Fig. 4). The model explained over 50 % of the annual biomass growth variance and 46 and 59 % of daily GPP in Fontblanche and Puechabon, respectively (Fig. 4). This means that we were able to mimic the seasonal and long-term trends in stand productivity with unbiased estimates but also to model how carbon is allocated to the stem along the year at the different phenophases described. The model assumed species-specific carbon allocation responses set to the different plant compartments as nonlinear functions of temperature and soil moisture. These relationships were biologically meaningful in the sense that photosynthesis and carbon allocation could be decoupled to some extent as a function of climatic variability. Once the canopy has been formed in spring, the model allocated more carbon to the stem and less to storage when less severe stress occurs, i.e. with decreasing temperatures and more humid conditions (Fig. 5).

Both sites exhibited an increase in temperature particularly evident in the maximum values but only Puechabon suffered a decrease in annual precipitation from 1960 to

2012 (Fig. A1). In the model, the studied forests acclimated to changing climatic conditions in the last decades coupling different physiological traits and simulated annual GPP greatly followed the overall trends in precipitation observed. In Fontblanche, which is milder and receives less precipitation, GPP remained stable since the 1960s and presented no apparent long-term trend. In contrast, in the coldest and rainiest site (Puechabon) the model simulated a decrease in GPP, which was likely driven by the prevailing decrease in precipitation observed since the 1960s (Fig. A1). This reduction of GPP should be partly a consequence of decreased LAI in response to enhanced long-term water stress (Fig. A3; Limousin et al., 2009; Misson et al., 2011). Simulated long-term decadal trends in mean annual stomatal conductance were similar and decreasing at the two sites likely as a consequence of enhanced temperatures (Fig. 6). The two species studied showed a long-term increase in simulated iWUE but not in ecosystem WUE (Fig. 7).

4 Discussion

4.1 Linking photosynthetic production to carbon allocation as a function of climate

The model calculates stand productivity and carbon allocation to stem growth in response to climate and [CO_2] with realism. It is particularly well suited to mimic the effect of water stress in plant performance by the explicit assessment of different acclimation processes including changes in stomatal conductance and leaf activity (Sala and Tenhunen, 1996; Reichstein et al., 2003; Limousin et al., 2010; Misson et al., 2011). Additionally, the model simulates carbohydrate storage dynamically as a function of environmental variability. Climate affects differently the carbon dynamics and allocation to different tree compartments at different phenophases. In the model the storage reservoir is an active sink for assimilated carbon during some periods of the year and a source in spring to be used in primary and secondary growth. This means that water stress and optimum temperature directly affect the modelled processes assuming that cell-wall expansion in the xylem can relate to climatic variability differently than photosynthesis. Therefore the C-source (photosynthesis) and the C-sink (growth) hypotheses can be assessed (Sala et al., 2012; Chen et al., 2013; Fatichi et al., 2014).

Water stress is generally considered the greatest limitation for Mediterranean ecosystems, driving an intimate relation between precipitation and both growth and photosynthesis (Breda et al., 2006; Pereira et al., 2007; Baldocchi et al., 2010; Gea-Izquierdo and Cañellas 2014). Our results show that a long-term decrease in precipitation would have triggered a decrease in simulated GPP at the more rainy and continental site. However, this decline was not expressed in the growth-trends. This means that long-term productivity and allocation of C to secondary growth were decoupled and did not match (Sala et al., 2012; Chen et al., 2013; Fatichi et al., 2014). The existence of trade-offs between carbon assimilation and allocation in relation to environmental variability suggests caution when using growth as a direct proxy to investigate stand productivity dynamics (Piovesan et al., 2008; Peñuelas et al., 2008; Gea-Izquierdo and Cañellas 2014). GPP was greater in the site receiving less precipitation, which could be related to differences in soil retention capacity. However both soils are calcareous, shallow and stony and differences in GPP could be also explained by less limitation for carbon assimilation of low winter temperatures. They can also be a result of different forest species composition (oak vs. pine-oak). LAI is greater at the site yielding higher annual GPP. Nonetheless, had this factor been responsible for the observed differences in winter photosynthesis, there would have also been differences in spring photosynthesis, which was not the case (Fig. 3).

A better understanding of the underlying processes determining carbon allocation will benefice process-based models (Sala et al., 2012; Fatichi et al., 2014). Model parameters were within the range found in the literature, bearing in mind that using a daily time step to study differential processes or not distinguishing between leaf ages will affect the scaling of parameters such as $J_{\mathrm{max}}/V_{\mathrm{cmax}}$ or R_{d} (De Pury and Farquhar, 1997; Grassi and Magnani, 2005; Masseyk et al., 2008; Vaz et al., 2010). Daily climatic data are readily available at a greater spatial scale than data with a higher temporal resolution, which increases applicability of daily models. Model performance could be improved by addressing respiration changes related to ontogeny and allometry, nutrient limitations (e.g. N/P) on photosynthesis, or including more complex up-scaling of leaf-level photosynthesis (Niinemets et al., 1999; Niinemets, 2007; Chen et al., 2013; McMurtrie and Dewar, 2013). However, it is difficult to find suitable data to calibrate such processes. Similarly, it would be challenging to include allocation to reproductive effort in the carbon budget. This is because, even if it is influenced by water stress in the studied forests (Pérez-Ramos et al., 2010), there is still great uncertainty in the causal factors driving multi-annual variability in fruit production (Koenig and Knops, 2000). Addressing stand dynamics would also help to generalize model applicability. Stand disturbances modifying stand competition can leave an imprint in growth for more than a decade whereas they do not seem to affect stand GPP over more than one or two years if the disturbance is moderate (Misson et al., 2005; Granier et al., 2008). In response to changes in competition the trees modify carbon allocation or keep the root : shoot ratio constant to enhance productivity on a per-tree basis but up to an asymptotic stand GPP. Still, the model behaviour was good compared with other studies that addressed ontogenic changes in the carbon-allocation response to photosynthesis (Li et al., 2014). Its behaviour was also similar or better than that of other mechanistic approaches calibrated to standardized dendroecological data (Misson et al., 2004; Evans et al., 2006; Gaucherel et al., 2008; Tolwinski-Ward et al., 2011; Touchan et al., 2012).

4.2 Forest performance in response to recent climate change and [CO_2] enhancement

Few studies under natural conditions observed a net increase of growth rates in response to enhanced CO_2 levels since the late 1800s, meaning that other factors such as water stress and N/P were more limiting for photosynthesis and allocation to growth than [CO_2] (Niinemets et al., 1999; Peñuelas et al., 2011; McMurtrie and Dewar, 2013;

Lévesque et al., 2014). Yet the forests have increased their iWUE. This can be partly a passive consequence of enhanced [CO_2] but higher iWUE observed in more water stressed sites suggests that climate is co-responsible of active acclimation physiological plant processes (Keenan et al., 2013; Leonardi et al., 2013; Silva and Horwarth, 2013; Saurer et al., 2014). These processes would include a higher stomatal control like in our results where in turn we did not observe any increase in long-term carbon assimilation. The mean annual stomatal conductance simulated was driven by climate but also decreased simultaneously in time with increasing [CO_2] (Fig. A4). Furthermore, there is debate on whether there has been an increase in ecosystem WUE in response to recent changes in [CO_2] under a warming climate (Beer et al., 2009; Reichstein et al., 2002; Keenan et al., 2013). We observed an increase in simulated annual WUE for the period 1980–2000 at the site where precipitation remained stable, whereas both sites showed a decrease in WUE since circa year 2000.

Higher CO_2 concentrations enhance photosynthesis with the equations used to calculate leaf photosynthesis in biochemical models (e.g. Gaucherel et al., 2008; Keenan et al., 2011; Leonardi et al., 2013; Boucher et al., 2014). Thus, the absence of a long-term increase in GPP and growth would not mean that enhanced [CO_2] was not beneficial for model outputs: growth and photosynthesis would have been lower had we used constant [CO_2] with the same model parameters. The absence of an enhancement in growth, even if there are changes in WUE, could express sink limitation related to hydraulic constraints (Peñuelas et al., 2011; Sala et al., 2012; Keenan et al., 2013). Often, the trees express a growth decline at those sites where there is an enhancement in long-term water stress that dominates species performance (e.g. Bigler et al., 2006; Piovesan et al., 2008). In contrast, it has been observed under certain conditions that trees have increased growth with warming since the 1850s (Salzer et al., 2009; Gea-Izquierdo and Cañellas 2014). These studies suggest the existence of a positive effect of warming rather than that of [CO_2] fertilization upon growth in forests where water stress is not the most limiting factor. Our study sites are located within the Northern limit of the Mediterranean Region, meaning that the two species studied occupy drier and warmer areas more to the South. Our results express the existence of trade-offs in response to climate at different phenological periods. This is important since synergistic environmental stresses acting at different periods can trigger tree mortality (McDowell et al., 2013; Voltas et al., 2013). Model sensitivity analysis could be performed to discuss the influence of specific factors such as climate or [CO_2] causing instability in the climate-growth response (D'Arrigo et al., 2008; Bouchard et al., 2014). However [CO_2] enhancement and climate warming are mixed in analysis performed using data from field studies, which can make the isolation of their effect problematic. The model can be applied using abundant dendrochronological data used to determine the site-dependent parameters. This would give much flexibility to investigate growth trends and forest performance in response to global change at a larger scale.

5 Conclusions

By developing an original process-based stand productivity model with climate explicit carbon allocation relationships we accurately simulated gross primary productivity and growth simultaneously in evergreen Mediterranean forests. Different processes were modelled as functions of environmental variability, including CO_2 and climate. The studied forests expressed trade-offs in carbon allocation to different plant compartments in response to stress in different seasons, namely winter low temperatures and photoperiod and summer moisture shortage. We modelled a decreasing time trend in stomatal conductance, which would suggest a partly active increase of iWUE in the forests studied. However, WUE decreased in recent years. Long-term GPP remained at similar levels in the last 50 years just in one stand whereas it declined in the forest suffering a reduction in precipitation. This suggests different acclimation processes to enhanced xericity and increasing CO_2 levels, which could not counterbalance the effect of warming just in one site. Tree growth was partly decoupled from stand productivity, highlighting that it can be risky to accept growth as a direct proxy to GPP. By calibrating a limited number of parameters related to carbon allocation the model has great potential to be used with abundant dendroecological data to characterise past instability in the growth response in relation to environmental variability and simulate future forest response under different climatic scenarios.

Acknowledgements. G. Gea-Izquierdo was funded by the Labex OT-Med (no. ANR-11-LABEX-0061) from the "Investissements d'Avenir" program of the French National Research Agency through the A*MIDEX project (no. ANR-11-IDEX-0001-02). Federation de Recherche FR3098 ECCOREV, the Labex IRDHEI and OHM-BMP also supported the study. We are grateful to Roland Huc for sharing data from Fontblanche.

References

Allard, V., Ourcival, J. M., Rambal, S., Joffre, R., and Rocheteau, A.: Seasonal and annual variation of carbon exchange in an evergreen Mediterranean forest in southern France, Glob. Change Biol., 14, 714–725, 2008.

Baldocchi, D. D.: Assessing the eddy covariance technique for evaluating carbon dioxide exchange rates of ecosystems: past, present and future. Glob. Change Biol., 9, 479–492, 2003.

Baldocchi, D. D., Ma, S. Y., Rambal, S., Misson, L., Ourcival, J. M., Limousin, J. M., Pereira, J., and Papale, D.: On the differential advantages of evergreenness and deciduousness in mediterranean oak woodlands: a flux perspective, Ecol. Appl., 20, 1583–1597, 2010.

Beer, C., Ciais, P., Reichstein, M., Baldocchi, D., Law, B. E., Papale, D., Soussana, J.-F., Ammann, C., Buchmann, N., Frank, D., Gianelle, D., Janssens, I. A., Knohl, A., Köstner, B., Moors, E., Roupsard, O., Verbeeck, H., Vesala, T., Williams, C. A., and Wohlfahrt, G.: Temporal and among-site variability of inherent water use efficiency at the ecosystem level, Global Biogeochem. Cy., 23, GB2018, 2009.

Bernacchi, C. J., Singsaas, E. L., Pimentel, C., Portis, A. R., and Long, S. P.: Improved temperature response functions for models of Rubisco-limited photosynthesis, Plant Cell Environ., 24, 253–259, 2001.

Bigler, C., Braker, O. U., Bugmann, H., Dobbertin, M., and Rigling, A.: Drought as an inciting mortality factor in Scots pine stands of the Valais, Switzerland, Ecosystems, 9, 330–343, 2006.

Boucher, É., Guiot, J., Hatté, C., Daux, V., Danis, P.-A., and Dussouillez, P.: An inverse modeling approach for tree-ring-based climate reconstructions under changing atmospheric CO_2 concentrations, Biogeosciences, 11, 3245–3258, doi:10.5194/bg-11-3245-2014, 2014.

Breda, N., Huc, R., Granier, A., and Dreyer, E.: Temperate forest trees and stands under severe drought: a review of ecophysiological responses, adaptation processes and long-term consequences, Ann. For. Sci., 63, 625–644, 2006.

Breshears, D. D., Myers, O. B., Meyer, C. W., Barnes, F. J., Zou, C. B., Allen, C. D., McDowell, N. G., and Pockman, W. T.: Tree die-off in response to global change-type drought: mortality insights from a decade of plant water potential measurements, Front. Ecol. Environ., 7, 185–189, 2009.

Chen, G., Yang, Y., and Robinson, D.: Allocation of gross primary production in forest ecosystems: allometric constraints and environmental responses, New Phytol., 200, 1176–1186, 2013.

D'Arrigo, R., Wilson, R., Liepert, B., and Cherubini, P.: On the "Divergence Problem" in Northern Forests: a review of the tree-ring evidence and possible causes, Global Planet. Change, 60, 289–305, 2008.

De Pury, D. G. G. and Farquhar, G. D.: Simple scaling of photosynthesis from leaves to canopies without the errors of big-leaf models, Plant Cell Environ., 20, 537–557, 1997.

De Kauwe, M. G., Medlyn, B. E., Zaehle, S., Walker, A. P., Dietze, M. C., Hickler, T., Jain, A. K., Luo, Y. Q., Parton, W. J., Prentice, I. C., Smith, B., Thornton, P. E., Wang, S. S., Wang, Y. P., Warlind, D., Weng, E. S., Crous, K. Y., Ellsworth, D. S., Hanson, P. J., Seok Kim, H., Warren, J. M., Oren, R., and Norby, R. J.: Forest water use and water use efficiency at elevated CO_2: a model-data intercomparison at two contrasting temperate forest FACE sites, Glob. Change Biol., 19, 1759–1779, 2013.

Dickman, L. T., McDowell, N. G., Sevanto, S., Pangle, R. E., and Pockman, W. T.: Carbohydrate dynamics and mortality in a piñon-juniper woodland under three future precipitation scenarios, Plant Cell Environ., doi:10.1111/pce.12441, 2014.

Evans, M. N., Reichert, B. K., Kaplan, A., Anchukaitis, K. J., Vaganov, E. A., Hughes, M. K., and Cane, M. A.: A forward modeling approach to paleoclimatic interpretation of tree-ring data, J. Geophys. Res., 111, G03008, doi:10.1029/2006JG000166, 2006.

Farquhar, G. D., von Caemmerer, S., and Berry, J. A.: A biochemical model of photosynthetic CO_2 assimilation in leaves of C3 species, Planta, 149, 78–90, 1980.

Fatichi, S., Leuzinger, S., and Körner, C.: Moving beyond photosynthesis: from carbon source to sink-driven vegetation modeling, New Phytol., 201, 1086–1095, 2013.

Flexas, J., Bota, J., Galmes, J., Medrano, H., and Ribas-Carbo, M.: Keeping a positive carbon balance under adverse conditions: responses of photosynthesis and respiration to water stress, Physiol. Plantarum, 127, 343–352, 2006.

Friedlingstein, P., Joel, G., Field, C. B., and Fung, I. Y.: Toward an allocation scheme for global terrestrial carbon models, Glob. Change Biol., 5, 755–770, 1999.

Fritts, H. C.: Tree Rings and Climate, Blackburn Press, New York, 567 pp., 1976.

Gaucherel, C., Campillo, F., Misson, L., Guiot, J., and Boreux, J. J.: Parameterization of a process-based tree-growth model: comparison of optimization, MCMC and Particle Filtering algorithms, Environ. Modell. Softw., 23, 1280–1288, 2008.

Gea-Izquierdo, G. and Cañellas, I.: Long-term climate forces instability in long-term productivity of a Mediterranean oak along climatic gradients, Ecosystems, 17, 228–241, 2014.

Gea-Izquierdo, G., Mäkelä, A., Margolis, H., Bergeron, Y., Black, T. A., Dunn, A., Hadley, J., Kyaw Tha Paw U, Falk, M., Wharton, S., Monson, R., Hollinger, D. Y., Laurila, T., Aurela, M., McCaughey, H., Bourque, C., Vesala, T., and Berninger, F.: Modeling acclimation of photosynthesis to temperature in evergreen conifer forests, New Phytol., 188, 175–186, 2010.

Granier, A., Breda, N., Longdoz, B., Gross, P., and Ngao, J.: Ten years of fluxes and stand growth in a young beech forest at Hesse, North-eastern France, Ann. For. Sci., 64, 704, 2008.

Grassi, G. and Magnani, F.: Stomatal, mesophyll conductance and biochemical limitations to photosynthesis as affected by drought and leaf ontogeny in ash and oak trees, Plant Cell Environ., 28, 834–849, 2005.

Guiot, J., Boucher, E., and Gea-Izquierdo, G.: Process models and model-data fusion in dendroecology, Front. Ecol. Evol., 2, 1–12, 2014.

Hoff, C. and Rambal, S.: An examination of the interaction between climate, soil and leaf area index in a Quercus ilex ecosystem, Ann. For. Sci., 60, 153–161, 2003.

IPCC: Climate Change: the Physical Science Basis, Summary for Policymakers, edited by: Stocker, T. F. et al., IPCC, Geneva, Switzerland, 33 pp., 2013.

Keenan, T., Maria Serra, J., Lloret, F., Ninyerola, M., and Sabate, S.: Predicting the future of forests in the Mediterranean under climate change, with niche- and process-based models: CO_2 matters!, Glob. Change Biol., 17, 565–579, 2011.

Keenan, T. F., Hollinger, D. Y., Bohrer, G., Dragoni, D., Munger, J. W., Schmid, H. P., and Richardson, A. D.: Increase in forest water-use efficiency as atmospheric carbon dioxide concentrations rise, Nature, 499, 324–327, 2013.

Koenig, W. D. and Knops, M. H.: Patterns of annual seed production by Northern Hemisphere trees: a global perspective, Am. Nat., 155, 59–69, 2000.

Leonardi, S., Gentilesca, T., Guerrieri, R., Ripullone, F., Magnani, F., Mencuccini, M., Noije, T. V., and Borghetti, M.: Assessing the effects of nitrogen deposition and climate on carbon isotope discrimination and intrinsic water-use efficiency of angiosperm and conifer trees under rising CO_2 conditions, Glob. Change Biol., 18, 2925–2944, 2012.

Le Roux, X., Lacointe, A., Escobar-Gutierrez, A., and Le Dizes, S.: Carbon-based models of individual tree growth: a critical appraisal, Ann. For. Sci., 58, 469–506, 2001.

Leuning, R.: A critical appraisal of a combined stomatal-photosynthesis model for C3 plants, Plant Cell Environ., 18, 339–355, 1995.

Lévesque, M., Siegwolf, R., Saurer, M., Eilmann, B., and Rigling, A.: Increased water-use efficiency does not lead to enhanced tree growth under xeric and mesic conditions, New Phytol., 203, 94–109, 2014.

Li, G., Harrison, S. P., Prentice, I. C., and Falster, D.: Simulation of tree-ring widths with a model for primary production, carbon allocation, and growth, Biogeosciences, 11, 6711–6724, doi:10.5194/bg-11-6711-2014, 2014.

Limousin, J. M., Rambal, S., Ourcival, J. M., Rocheteau, A., Joffre, R., and Rodriguez-Cortina, R.: Long-term transpiration change with rainfall decline in a Mediterranean *Quercus ilex* forest, Glob. Change Biol., 15, 2163–2175, 2009.

Limousin, J. M., Longepierre, D., Huc, R., and Rambal, S.: Change in hydraulic traits of Mediterranean *Quercus ilex* subjected to long-term throughfall exclusion, Tree Physiol., 30, 1026–1036, 2010.

Limousin, J.-M., Rambal, S., Ourcival, J.-M., Rodriguez-Calcerrada, J., Perez-Ramos, I. M., Rodriguez-Cortina, R., Misson, L., and Joffre, R.: Morphological and phenological shoot plasticity in a Mediterranean evergreen oak facing long-term increased drought, Oecologia, 169, 565–577, 2012.

Maseyk, K. S., Lin, T., Rotenberg, E., Grünzweig, J. M., Schwartz, A., and Yakir, D.: Physiology-phenology interactions in a productive semi-arid pine forest, New Phytol., 178, 603–16, 2008.

McDowell, N. G., Fisher, R. A., Xu, C., Domec, J., Höltta, T., Mackay, D. S., Sperry, J. S., Boutz, A., Dickman, L., Gehres, N., Limousin, J. M., Macalady, A., Pangle, R. E., Rasse, D. P., Ryan, M. G., Sevanto, S., Waring, R. H., Williams, A. P., Yepez, E. A., and Pockman, W. T.: Evaluating theories of drought-induced vegetation mortality using a multimodel – experiment framework, New Phytol., 200, 304–321, 2013.

McMurtrie, R. E. and Dewar, R. C.: New insights into carbon allocation by trees from the hypothesis that annual wood production is maximized, New Phytol., 199, 981–990, 2013.

Misson, L.: MAIDEN: a model for analyzing ecosystem processes in dendroecology, Can. J. Forest Res., 34, 874–887, 2004.

Misson, L., Rathgeber, C., and Guiot, J.: Dendroecological analysis of climatic effects on Quercus petraea and Pinus halepensis radial growth using the process-based MAIDEN model, Can. J. Forest Res., 34, 888–898, 2004.

Misson, L., Tang, J., Xu, M., Mckay, M., and Goldstein, A.: Influences of recovery from clear-cut, climate variability, and thinning on the carbon balance of a young ponderosa pine plantation, Agric. For., 130, 207–222, 2005.

Misson, L., Degueldre, D., Collin, C., Rodriguez, R., Rocheteau, A., Ourcival, J.-M., and Rambal, S.: Phenological responses to extreme droughts in a Mediterranean forest, Glob. Change Biol., 17, 1036–1048, 2011.

Montserrat-Marti, G., Camarero, J. J., Palacio, S., Perez-Rontome, C., Milla, R., Albuixech, J., and Maestro, M.: Summer-drought constrains the phenology and growth of two coexisting Mediterranean oaks with contrasting leaf habit: implications for their persistence and reproduction, Trees-Struct. Funct., 23, 787–799, 2009.

Niinemets, U.: Photosynthesis and resource distribution through plant canopies, Plant Cell Environ., 30, 1052–1071, 2007.

Niinemets, U. and Valladares, F.: Photosynthetic acclimation to simultaneous and interacting environmental stresses along natural light gradients: optimality and constraints, Plant Biol., 6, 254–68, 2004.

Niinemets, Ü., Tenhunen, J. D., Canta, N. R., Chaves, M. M., Faria, T., Pereira, J. S., and Reynolds, J. F.: Interactive effects of nitrogen and phosphorus on the acclimation potential of foliage photosynthetic properties of cork oak, *Q. suber*, to elevated atmospheric CO_2 concentrations, Glob. Change Biol., 5, 455–470, 1999.

Nobel, P. S.: Physicochemical and Environmental Plant Physiology, 4th edn., Academic Press, Elsevier, Oxford, UK, 2009.

Peng, C. H., Guiot, J., Wu, H. B., Jiang, H., and Luo, Y. Q.: Integrating models with data in ecology and palaeoecology: advances towards a model-data fusion approach, Ecol. Lett., 14, 522–536, 2011.

Peñuelas, J., Hunt, J. M., Ogaya, R., and Jump, A. S.: Twentieth century changes of tree-ring delta C-13 at the southern range-edge of *Fagus sylvatica*: increasing water-use efficiency does not avoid the growth decline induced by warming at low altitudes, Glob. Change Biol., 14, 1076–1088, 2008.

Peñuelas, J., Canadell, J. G., and Ogaya, R.: Increased water-use efficiency during the 20th century did not translate into enhanced tree growth, Global Ecol. Biogeogr., 20, 597–608, 2011.

Pereira, J. S., Mateus, J. A., Aires, L. M., Pita, G., Pio, C., David, J. S., Andrade, V., Banza, J., David, T. S., Paço, T. A., and Rodrigues, A.: Net ecosystem carbon exchange in three contrasting Mediterranean ecosystems – the effect of drought, Biogeosciences, 4, 791–802, doi:10.5194/bg-4-791-2007, 2007.

Pérez-Ramos, I. M., Ourcival, J. M., Limousin, J. M., and Rambal, S.: Mast seeding under increasing drought: results from a long-term data set and from a rainfall exclusion experiment, Ecology, 91, 3057–3068, 2010.

Piovesan, G., Biondi, F., Di Filippo, A., Alessandrini, A., and Maugeri, M.: Drought-driven growth reduction in old beech (*Fagus sylvatica* L.) forests of the central Apennines, Italy, Glob. Change Biol., 14, 1265–1281, 2008.

Rambal, S., Joffre, R., Ourcival, J. M., Cavender-Bares, J., and Rocheteau, A.: The growth respiration component in eddy CO_2 flux from a *Quercus ilex* mediterranean forest, Glob. Change Biol., 10, 1460–1469, 2004.

Reichstein, M., Tenhunen, J. D., Roupsard, O., Ourcival, J. M., Rambal, S., Miglietta, F., Peressotti, A., Pecchiari, M., Tirone, G., and Valentini, R.: Severe drought effects on ecosystem CO_2 and H_2O fluxes at three Mediterranean evergreen sites: revision of current hypotheses?, Glob. Change Biol., 6, 999–1017, 2002.

Reichstein, M., Tenhunen, J., Roupsard, O., Ourcival, J. M., Rambal, S., Miglietta, F., Peressotti, A., Pecchiari, M., Tirone, G., and Valentini, R.: Inverse modeling of seasonal drought effects on canopy CO_2/H_2O exchange in three Mediterranean ecosystems, J. Geophys. Res., 108, 20, 2003.

Reichstein, M., Falge, E., Baldocchi, D., Papale, D., Aubinet, M., Berbigier, P., Bernhofer, C., Buchmann, N., Gilmanov, T., Granier, A., Grunwald, T., Havrakova, K., Ilvesniemi, H., Janous, D., Knohl, A., Laurila, T., Lohila, A., Loustau, D., Matteucci, G., Meyers, T., Miglietta, F., Ourcival, J. M., Pumpanen, J., Rambal, S., Rotenberg, E., Sanz, M., Tenhunen, J., Seufert, G., Vaccari, F., Vesala, T., Yakir, D., and Valentini, R.: On the separation of net ecosystem exchange into assimilation and ecosystem respiration: review and improved algorithm, Glob. Change Biol., 11, 1424–1439, 2005.

Sala, A. and Tenhunen, J. D.: Simulations of canopy net photosynthesis and transpiration in *Quercus ilex* L. under the influence of seasonal drought, Agr. Forest Meteorol., 78, 203–222, 1996.

Sala, A., Woodruff, D. R., and Meinzer, F. C.: Carbon dynamics in trees: feast or famine?, Tree Physiol., 32, 764–75, 2012.

Salzer, M. G., Hughes, M. K., Bunn, A. G., and Kipfmueller, K. F.: Recent unprecedented tree-ring growth in bristlecone pine at the highest elevations and possible causes, P. Natl. Acad. Sci. USA, 106, 20348–20353, 2009.

Saurer, M., Spahni, R., Frank, D. C., Joos, F., Leuenberger, M., Loader, N. J., McCarroll, D., Gagen, M., Poulter, B., Siegwolf, R. T. W., Andreu-Hayles, L., Boettger, T., Dorado, I., Fairchild, I. J., Friedrich, M., Gutierrez, E., Haupt, M., Hilasvuori, E., Heinrich, I., Helle, G., Grudd, H., Jalkanen, R., Levanič, T., Linderholm, H. W., Robertson, I., Sonninen, E., Treydte, K., Waterhouse, J. S., Woodley, E. J., Wynn, P. M., and Young, G. H. F.: Spatial variability and temporal trends in water-use efficiency of European forests, Glob. Change Biol., 3700–3712, 2014.

Schaefer, K., Schwalm, C. R., Williams, C., Arain, M. A., Barr, A., Chen, J. M., Davis, K. J., Dimitrov, D., Hilton, T. W., Hollinger, D. Y., Humphreys, E., Poulter, B., Raczka, B. M., Richardson, A. D., Sahoo, A., Thornton, P., Vargas, R., Verbeeck, H., Anderson, R., Baker, I., Black, T. A., Bolstad, P., Chen, J., Curtis, P. S., Desai, A. R., Dietze, M., Dragoni, D., Gough, C., Grant, R. F., Gu, L., Jain, A., Kucharik, C., Law, B., Liu, S., Lokipitiya, E., Margolis, H. A., Matamala, R., McCaughey, J. H., Monson, R., Munger, J. W., Oechel, W., Peng, C., Price, D. T., Ricciuto, D., Riley, W. J., Roulet, N., Tian, H., Tonitto, C., Torn, M., Weng, E., and Zhou, X.: A model-data comparison of gross primary productivity: results from the North American Carbon Program site synthesis, J. Geophys. Res., 117, G03010, doi:10.1029/2012JG001960, 2012.

Silva, L. C. R. and Horwath, W. R.: Explaining global increases in water use efficiency: why have we overestimated responses to rising atmospheric CO_2 in natural forest ecosystems?, PLoS One, 8, e53089, doi:10.1371/journal.pone.0053089, 2013.

Simioni, G., Durand-Gillmann, M., and Huc, R.: Asymmetric competition increases leaf inclination effect on light absorption in mixed canopies, Ann. For. Sci., 70, 123–131, 2013.

Tolwinski-Ward, S. E., Evans, M. N., Hughes, M. K., and Anchukaitis, K. J.: An efficient forward model of the climate controls on interannual variation in tree-ring width, Clim. Dynam., 36, 2419–2439, 2011.

Touchan, R., Shishov, V. V., Meko, D. M., Nouiri, I., and Grachev, A.: Process based model sheds light on climate sensitivity of Mediterranean tree-ring width, Biogeosciences, 9, 965–972, doi:10.5194/bg-9-965-2012, 2012.

Vaganov, E. A., Hughes, M. K., and Shashkin, A. V.: Growth Dynamics of Conifer Tree Rings: Images of Past and Future Environments, Springer, New York, 2006.

Vaz, M., Pereira, J. S., Gazarini, L. C., David, T. S., David, J. S., Rodrigues, A., Maroco, J., and Chaves, M. M.: Drought-induced photosynthetic inhibition and autumn recovery in two Mediterranean oak species (*Quercus ilex* and *Quercus suber*), Tree Physiol., 30, 946–956, 2010.

Voltas, J., Camarero, J. J., Carulla, D., Aguilera, M., Ortiz, A., and Ferrio, J. P.: A retrospective, dual-isotope approach reveals individual predispositions to winter-drought induced tree dieback in the southernmost distribution limit of Scots pine, Plant. Cell Environ., 36, 1435–1448, 2013.

Title Page
Abstract | Introduction
Conclusions | References
Tables | Figures
◀◀ | ▶▶
◀ | ▶
Back | Close
Full Screen / Esc
Printer-friendly Version
Interactive Discussion

Table 1. Characteristics of mean annual gross primary productivity, climatic (annual means) and growth data. SDs are shown between parentheses. Precipitation = mean annual precipitation; T_{max} = annual mean of mean daily maximum temperature; T_{min} = annual mean of mean daily minimum temperature. Length = chronology year replicated with more than 5 radii; RW = mean annual ring-width; Rbs = mean correlation between series; AR = mean autocorrelation of raw series; MS = mean sensitivity; EPS = mean expressed population signal Rbs, AR, MS and EPS are classical statistics to characterise growth chronologies, and follow Fritts (1976).

		Fontblanche		Puechabon
Flux Data	Period	2008–2012		2001–2013
	GPP annual ($\mathrm{g\,C\,m^{-2}\,year^{-1}}$)	1431.4 (305.4)		1207.3 (206.7)
Climate	Period	1964–2012		1954–2013
	Precipitation (mm)	642.7 (169.7)		1002.6 (328.2)
	T_{max} (°C)	20.6 (0.9)		17.8 (1.26)
	T_{min} (°C)	8.8 (0.5)		8.1 (0.8)
Growth Data	Species	*P. halepensis*	*Q. ilex*	*Q.ilex*
	# Trees/Radii	25/47	15/30	17/32
	Length	1910–2013	1941–2013	1941–2005
	RW (mm)	2.19 (1.1)	1.25 (0.7)	1.13 (0.7)
	MS	0.308	0.372	0.443
	AR	0.684	0.591	0.436
	Rbs	0.541	0.281	0.457
	EPS	0.963	0.884	0.949

Title Page
Abstract | Introduction
Conclusions | References
Tables | Figures
◀| |▶
◀ ▶
Back | Close
Full Screen / Esc
Printer-friendly Version
Interactive Discussion

Table 2. Model parameters. Those parameter differing between sites were optimized either with GPP data (photosynthesis and allocation module) or with growth-based biomass increment chronologies (allocation module). The rest were common parameters for both sites and selected while developing the model in the first step for Fontblanche using GPP data (represented in "Cal" with a "–"). Meaning of parameters, equation number (E#) and phenophase [P#] are as in the text in Material and Methods. Fontb = Fontblanche; Puech = Puechabon; Cal = local parameters to be calibrated with GPP or stem biomass increment data (SBI).

Process	Process/Equation #	Parameter		Fontb	Puech	Units	Cal
Photosynthesis	Leaf photosynthesis (Eq. 2)	J_{coef}	QUIL	1.59		μmol C m^2 s^{-1}	–
			PIHA	1.44	–		
	Leaf photosynthesis (Eq. 3)	$V_{\max}$	QUIL	32.3		μmol C m^2 s^{-1}	–
			PIHA	46.0	–		
		V_b	QUIL	−0.106		°C^{-1}	–
			PIHA	−0.180	–		
		V_{ip}	QUIL	13.7		°C	–
			PIHA	20.0	–		
	Stress V_{cmax} (Eq. 4)	p_{str}		−0.05		mm^{-1}	–
	Stomatal conductance (Eq. 5)	g_1	QUIL	7.5		–	–
			PIHA	6.1	–		
		VPD_0		30 000		Pa	–
	Water stress (Eq. 6)	Soil_b		−0.054		mm^{-1}	–
		Soil_{ip}		22.2	81.8	mm	GPP
Allocation	Respiration (Eq. 7)	p_{respi}		−0.225		°C^{-1}	–
	Stress LAI (Eq. 8)	p_{LAI}		65.5		mm	–
	[P2]	GDD_1		203.3		°C	–
	Stored carbon buds [P3]	C_{bud}		7		g C day^{-1}	–
	[P5]	Photoperiod		9.5		hours	–
	Allocation canopy [P3], (Eq. 9)	$\text{st}_{4\text{moist}}$		−0.089	−0.173	mm^{-1}	GPP
		$\text{st}_{4\text{temp}}$		53.3	75	°C	GPP
		$\text{st}_{4\text{sd}}$		26.9	26.1	°C	GPP
	Allocation stem [P3], (Eq. 10)	$\text{st}_{3\text{moist}}$		−0.045	−0.117	mm^{-1}	SBI
		$\text{st}_{3\text{temp}}$		32.9	6.3	°C	SBI
		$\text{st}_{3\text{sd}}$		38.0	3.0	°C	SBI
	Allocation stor/stem [P4], (Eq. 11)	$\text{st}_{4\text{moist}}$		200.8	119.3	mm	SBI
		$\text{st}_{4\text{temp}}$		0.060	−0.097	°C^{-1}	SBI

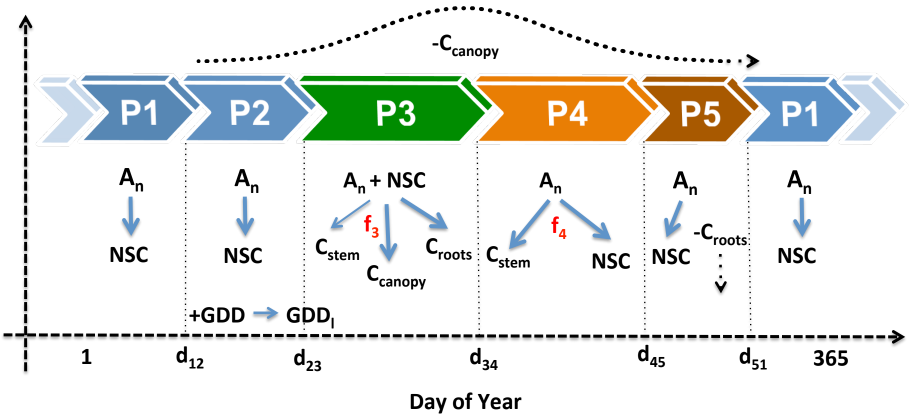

Figure 1. Outline of the different phenological phases (P1 to P5) and carbon allocation in the model within a given year. A_n = net daily carbon assimilation; NSC = storage (non-structural carbohydrates); GDD = growing degree days, GDD$_l$ = parameter determining shift from P2 to P3 (see text); C = carbon allocated either to the stem, canopy or roots; d = day of year. Solid arrows correspond to allocation within the plant whereas dashed arrows to correspond to litter-fall (canopy or roots). f_3 and f_4 are nonlinear functions of soil water content and temperature determining carbon allocation to different compartments (see text for more details).

Title Page
Abstract
Introduction
Conclusions
References
Tables
Figures
◀◀
▶▶
◀
▶
Back
Close
Full Screen / Esc
Printer-friendly Version
Interactive Discussion

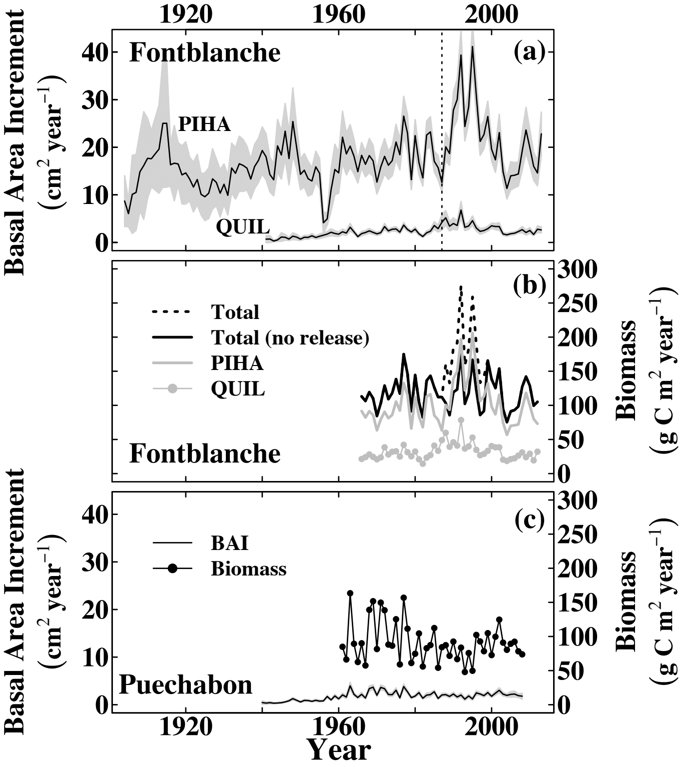

Figure 2. Growth (basal area increment, BAI, cm^2 year^{-1}) and biomass allocated to the tree stem (g C m^{-2} year^{-1}) of *Q. ilex* and *P. halepensis* at Fontblanche (growth shown in **(a)**, biomass in **(b)**) and *Q. ilex* at Puechabon (growth and stem biomass shown in **(c)**). A vertical dashed line marks the release event in Fontblanche produced by enhanced winter mortality in 1985 in **(a)**. Dark lines for BAI correspond to yearly means while grey polygons show confidence intervals on the standard errors of the mean.

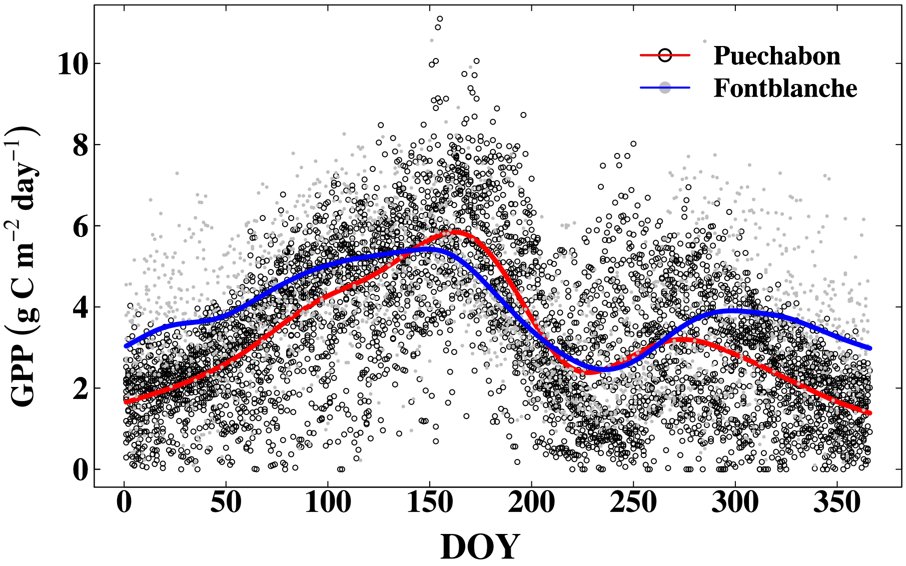

Figure 3. Daily gross primary productivity (GPP) at Puechabon (2001–2013, black dots, red line) and Fontblanche (2008–2012, grey dots, blue line). DOY = day of year. Thick lines correspond to smoothers fitted to the mean to highlight seasonal trends at the two sites.

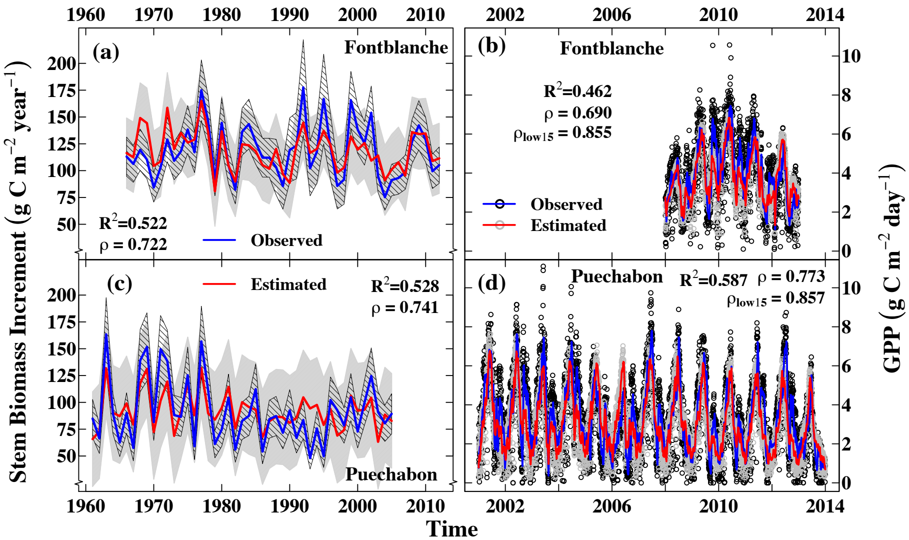

Figure 4. Model fit to stem biomass increment **(a)** and GPP **(b)** in Fontblanche; and stem biomass increment **(c)** and GPP **(d)** in Puechabon. R^2 = coefficient of determination; ρ = linear correlation between estimated and observed data, ρ_{low15} = linear correlation between estimated and observed data smoothed with a 15 year low-pass filter (blue and red lines in **(b)** and **(c)**). Polygons behind the estimated values in **(a)** and **(c)** correspond to confidence intervals of the mean: solid grey polygons for estimated values and dashed polygons for observed stem biomass increment values.

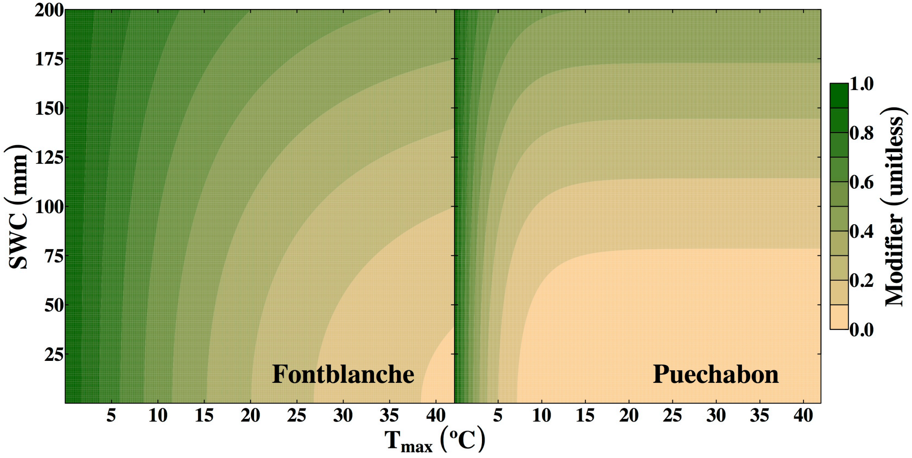

Figure 5. Modelled carbon allocation trajectory to the stem after leaf flush has finished in phenological period [P4]. We show the unitless modifier $1-h_4(i)$ (i.e. $h_4(i)$ is the portion of allocated carbon to storage) from $C_{\text{stem}}(i) = A_{\text{N}}(i) \cdot [(1-h_4(i))]$ as from Eq. (11). The modifier [0, 1] is a function of soil water content (SWC) and maximum temperature (T_{max}) and multiplies available daily carbon to distribute daily carbon allocated between secondary growth and storage.

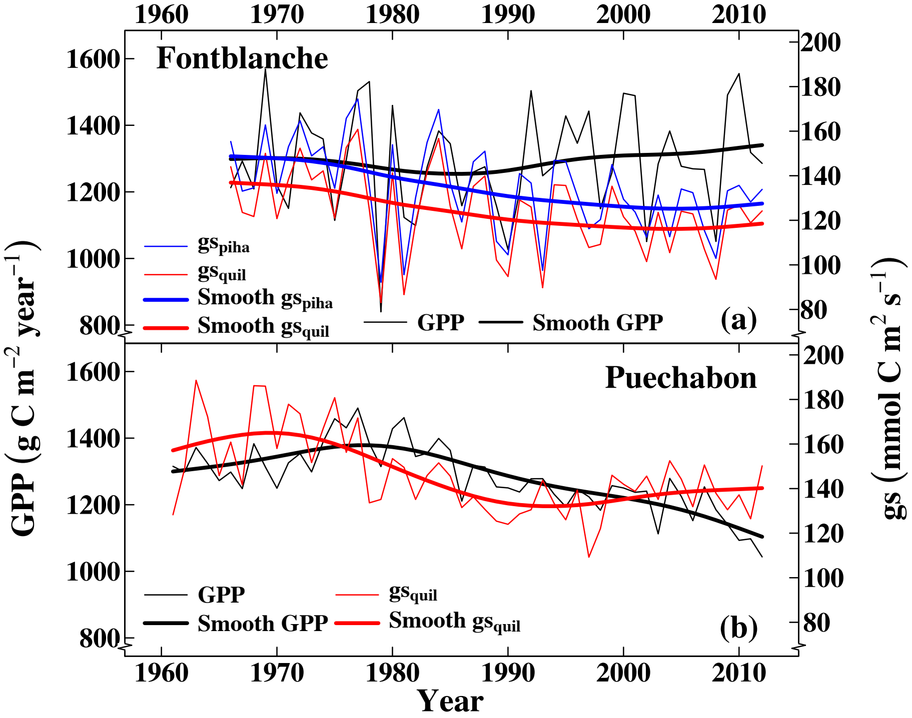

Figure 6. Modelled total annual stand gross primary productivity (GPP) and mean stomatal conductance of sunny leaves (gs) for Fontblanche **(a)** and Puechabon **(b)** for the period where meteorological data were available.

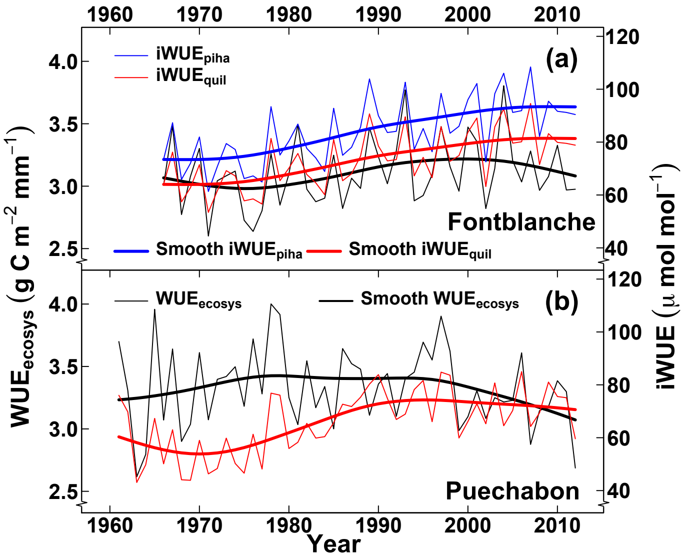

Figure 7. Ecosystem WUE (integral annual) and iWUE for sun leaves (mean daily, for PIHA and QUIL separated in Fontblanche) for **(a)** Fontblanche and **(b)** Puechabon for the period where we had available meteorological data.

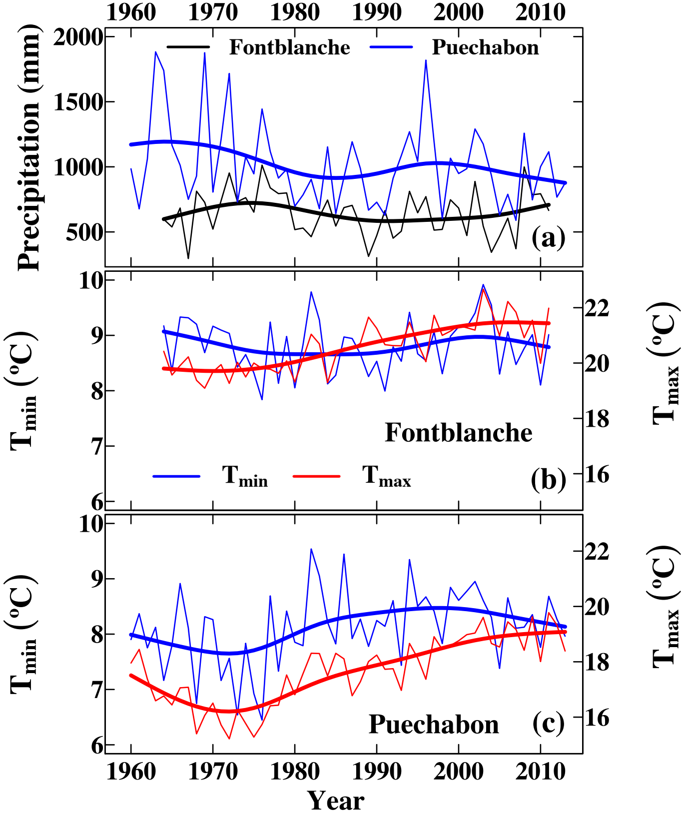

Figure A1. Mean climatic time series in the last 50 years. **(a)** Annual precipitation; **(b)** and **(c)** annual maximum (T_{max}) and minimum (T_{min}) temperatures for Fontblanche **(b)** and Puechabon **(c)**.

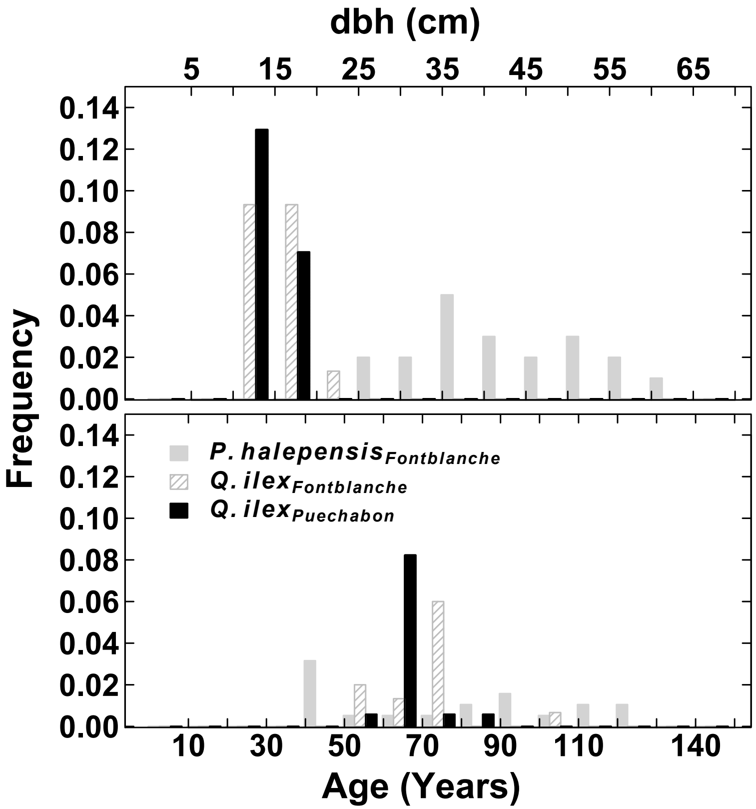

Figure A2. Diameter (dbh, cm) and age (years) distribution of trees included in the chonologies. Frequencies are calculated separately by species and site.

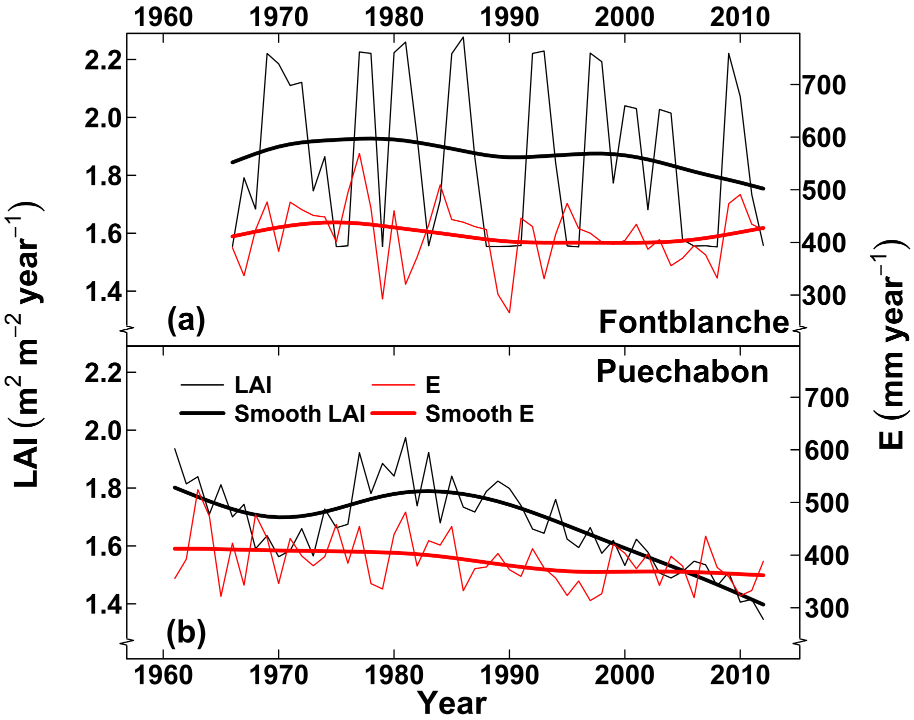

Figure A3. Simulated maximum annual leaf area index LAI (m^2 m^{-2}) and total annual stand transpiration E (mm year^{-1}) in Fontblanche **(a)** and Puechabon **(b)**.

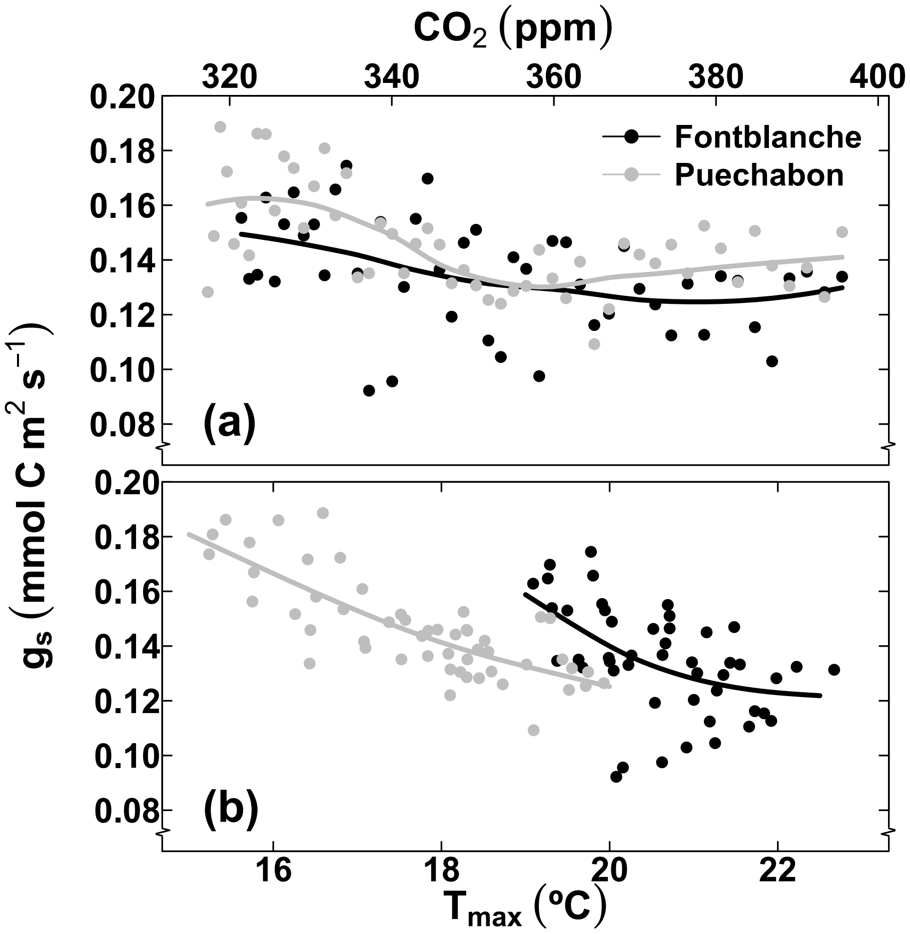

Figure A4. Simulated mean annual stomatal conductance (g_s) as a function of mean [CO$_2$] **(a)** and mean maximum temperature **(b)**.